

Synthesis and Nonlinear-Optical Properties of Vinyl-Addition Poly(norbornene)s

Ki Hong Park,^{†,‡} Robert J. Twieg,^{*,†} R. Ravikiran,[§] Larry F. Rhodes,^{*,§} Robert A. Shick,[§] Diego Yankelevich,[‡] and Andre Knoesen[‡]

Chemistry Department, Kent State University, Kent, Ohio 44240, Promerus LLC, 9921 Brecksville Road, Brecksville, Ohio 44141, and Department of Electrical and Computer Engineering, University of California at Davis, Davis, California 95616

Received February 23, 2004; Revised Manuscript Received April 27, 2004

ABSTRACT: Vinyl-addition poly(norbornene) copolymers functionalized with nonlinear optical chromophore side groups have been prepared using (η^6 -toluene)Ni(C₆F₅)₂, and their electrooptic properties have been characterized. The nickel complex used to polymerize the norbornene monomers is tolerant to many functional groups found in nonlinear optical chromophores although nitriles and amines other than trisubstituted amines strongly inhibit the reaction. A vinyl-addition copolymer of hexylnorbornene and a norbornene-functionalized Disperse Red 1 chromophore was scaled up and studied in detail. Initial studies indicate that electric field poling is effective but that relaxation of polar order in the poly(norbornene) is faster than in a comparable methacrylate copolymer.

Introduction

Information processing and telecommunications technologies are approaching a barrier to meet current much less anticipated demands of signal propagation and switching speeds available based solely on electronics. As a result, the future ultrafast computing and communications systems will inevitably integrate photonics on a much larger scale. For such optical communication networks, one of the critical components required is the optical fiber by which data is relayed. Another critical component is an optical modulator or switch required to put the information on and off the fiber and to route the information. In existing optical networks, these components rely heavily on silica to provide the information transport function and on lithium niobate to provide the information switching and routing function, although numerous other schemes and materials have also been proposed and studied. In the case of the switching and routing function, organic and polymer electrooptical media that can emulate lithium niobate (and eventually have performance superior to lithium niobate) have been the most intensively investigated.¹ This sustained study has been motivated by the conviction that these polymers can provide a cost-effective solution due to their intrinsic design and processing flexibility. Furthermore, in addition to applications in computing and communications, such polymeric nonlinear optical (NLO) media may find additional utility in photorefractive systems, phase array radar, and many other related applications.

Over the past 2 decades significant progress has been made, leading to the design and fabrication of more practical and reliable organic and polymeric photonics materials and devices. Even in the area of electrooptics alone, an enormous variety of nonlinear chromophores

and host polymers in numerous combinations have been examined with very mixed results. To date, there still seems to be no general consensus on any unique design strategy that leads to the simultaneous optimization of all the required and often seemingly incompatible physical properties demanded of a single clearly superior electrooptic material. This should probably be no surprise given the inherent complexity of the problem at hand and also given the diverse options that organic chemistry and polymer science present as potential solutions. The matrix of possibilities is huge. Consider first that the “magic bullet” chromophore (with a large molecular $\mu\beta$ product, miscibility, and other properties leading to creation of sufficient nonlinear susceptibility $\chi^{(2)}$ manifested as a large electrooptic coefficient r_{33} , a small V_{π} , and last but not never least, sufficient photochemical and thermochemical stability) remains to be identified. Next, consider the myriad of permutations on the polymer class to select from (acrylate, polyimide, polyquinoline, sol-gel, epoxy, etc.) and then, finally, the exact relationship between the chromophore and polymer (guest-host, covalent main-chain, covalent side-chain, linear, dendrimer, nonfunctionalized and nonreactive, functionalized and reactive, etc.). The choice of the appropriate NLO polymer is one beset by many tradeoffs. On one hand the relative ease and compatibility in processing polymers is promoted as a great asset. On the other hand, this enhanced processability tends to compromise (but not negate) the achievement of large and stable polar order. Therefore, one critical issue in NLO polymeric material has been the enhancement of long-term stability of NLO properties. Unlike inorganic materials, where the polar order is “built in”, in the case of polymers the NLO chromophores (the donor-bridge-acceptor unit) must be oriented (poled) by an external electric field and this polar order must be retained even at elevated temperatures in the absence of that poling field. Therefore, it is very important to sustain the polar alignment of NLO chromophores in the polymer matrix for a long period. For this reason, high glass temperature (T_g) polymers such as polyimides have been proposed as suitable NLO

* To whom correspondence should be addressed. E-mail: larry.rhodes@promerus.com.

[†] Kent State University.

[‡] Current address: KIST, Electronic Materials & Devices Research Center, Seoul, 130-650, Korea.

[§] Promerus LLC.

[‡] University of California at Davis.

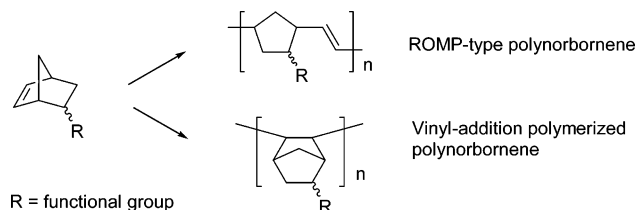


Figure 1. Ring opening metathesis type vs vinyl-addition type polymerization.

polymer backbones. However, the large birefringence associated with many polyimides make them as a class of materials less than ideal for electrooptics. As an alternative, cross-linking strategies have been examined to freeze in polar order by creation of new chemical bonds that might better lock chromophores in a polar arrangement.²

A class of polymers that exhibit very good optical properties including low birefringence are poly(cyclic olefins). Ring-opening polymerization of cyclic olefins, such as norbornene, give ROMP-type polymers (Figure 1). However, these types of polymers exhibit T_g 's that are significantly lower (typically below 200 °C) than polyimides and they suffer from thermooxidative instability due to the presence of unsaturation in the backbone. Despite these potential problems, there have been a few brief reports about application of ROMP systems as nonlinear optical polymers (NLOP)^{3,4} and as other kinds of optical and electronic materials such as side chain liquid crystals (SCLCP),⁵ electroluminescent materials (EL),⁶ and organic light emitting diode (OLED).⁷

Another method of preparing cyclic olefin polymers is by vinyl addition polymerization (Figure 1). Vinyl addition polymers of norbornene were originally reported as early as 1963.^{8a} A report of vinyl addition polymerization of functional norbornenes appeared in 1967.^{8b} Since then there have been a number of reports describing early transition metal metallocene and late transition metal catalysts for their preparation.⁹ The vinyl-polymerized norbornenes synthesized using certain metallocenes were found to be highly tactic, high melting, semicrystalline materials that would seem to be unsuitable for optical applications.¹⁰ Those polymers produced by late transition metals were found to be less stereoregular. Recently, new group VIII transition metal catalyst systems for the vinyl addition polymerization of norbornene-type monomers have appeared.¹¹ These addition-type poly(norbornene)s have high T_g 's in the range of about 180–370 °C depending on the type of pendant groups (R) attached to the norbornene, whereas the highly unsaturated ring-opening metathesis polymerization (ROMP) polymer of the parent norbornene has a T_g of only about 35 °C.¹² Furthermore, addition-type poly(norbornene)s are amorphous, exhibit low birefringence and can exhibit low moisture absorption.¹³ They are also more thermally stable than the corresponding ROMP polymers since they contain no unsaturation. Recently, photochromic poly(norbornene)s have been successfully synthesized by this vinyl addition polymerization method.¹⁴

This investigation describes our preliminary attempts to exploit vinyl-addition polymerized poly(norbornene) as a new polymer class for NLO applications. Here we demonstrate the preparation of norbornene monomers functionalized with some conventional NLO chromophores and their successful polymerization with (η^6 -

toluene)Ni(C₆F₅)₂ to give the chromophore-functionalized poly(norbornene)s. We also report preliminary nonlinear optical measurements on one of the new NLO polymers we have prepared.

Experimental Section

Materials. Starting materials for chromophore synthesis including 4-aminobenzonitrile (**1**), 2-(*N*-ethylamino)ethanol (**2**), 4-nitrophenylacetic acid (**4**), 6-chloro-1-hexanol (**6**), 4-*N,N*-(diethylamino)salicylaldehyde (**7**), ethyl cyanoacetate (**9**), isophorone (**10**), 4-*N,N*-dimethylaminobenzaldehyde (**12**), and Disperse Red 1 (**C1**) were purchased from the Aldrich Chemical Co. The 1,5,5-trimethylcyclohex(2-enylidene)malononitrile (**5**) was provided by IBM Almaden Research Laboratory for research use. The dibutyltin oxide (98%) was purchased from Acros Organics. The 5-norbornene-2-ethyl ester (**13**), 5-norbornene-2-methanol (**14**), and 5-norbornene-2-hexyl monomers (**18**) were provided by the BFGoodrich Co. Anhydrous toluene (99.8%) used as a polymerization solvent was purchased from Aldrich. (η^6 -toluene)Ni(C₆F₅)₂ was prepared according to a literature method.¹⁵ The DR1-PMMA copolymer used in this study for comparative purposes was obtained from the IBM Almaden Research Laboratory.¹⁶

Measurements. Chemical Characterization. Routine ¹H NMR spectra were obtained on a Bruker AMX300 NMR (300 MHz) spectrometer while a Varian Inova 500 MHz spectrometer MHz spectrometer was used for ¹H NMR examination of the polymer samples. The maximum absorption wavelengths (λ_{max}) of compounds were determined by HP 8453 UV-visible spectrophotometer in acetonitrile (CH₃CN). The melting points (peak points and onset points) of all synthesized compounds were measured on TA Instruments 2920 DSC at a heating rate of 5 °C/min under nitrogen. Molecular weight measurements were determined by gel-permeation chromatography (GPC) using a refractive index detector. Polymer samples were dissolved in stabilized THF (50 mg/20 mL) and filtered through a 0.20 μ m Teflon filter. All the molecular weights are measured relative to polystyrene standards. Dynamic mechanical analysis (DMA) experiments were done using a Rheometrics RSA II analyzer as per the ASTM D5026-95a method (DMA of plastics in tension). The polymer films were heated in 3° C steps with the dwell time at each temperature being 1 min. Polymer samples for DMA were prepared by casting a solution of the polymer (in mesitylene) onto a glass plate and allowing the solvent to evaporate overnight. The films were then baked at 200 °C under vacuum to ensure complete removal of solvent.

Nonlinear Optical Characterization. Thin films were prepared by spin casting polymer solutions onto a soda-lime glass substrate followed by baking to remove residual solvent. The film thickness was measured by contact profilometry. The second harmonic generation (SHG) measurements were performed using a p-polarized Q-switched Nd:YLF laser beam incident at Brewster's angle on the surface coated with the electrooptic polymer. The laser operates at a wavelength of 1057 nm with a 1 kHz repetition rate. The generated second harmonic and fundamental beams are filtered using dichroic mirrors and filters. The second harmonic signal is detected with a PMT and lock-in amplifier. The average fundamental power was kept constant throughout the measurements as verified with a pyroelectric power meter. The refractive index as a function of wavelength was measured by variable angle spectroscopic ellipsometry.

Assuming a simple scalar model, the macroscopic dielectric polarizability is

$$P \approx \epsilon_0 \chi^{(1)} E + \epsilon_0 \chi^{(2)} E^2 + \epsilon_0 \chi^{(3)} E^3$$

where $\chi^{(1)}$, $\chi^{(2)}$, and $\chi^{(3)}$ are the macroscopic linear polarizability, second-order nonlinear polarizability, and the third-order nonlinear polarizability, respectively. If the applied electric field consists of a strong static electric field E_0 and an optical beam $E_1 \cos(\omega t)$, then substituting $E = E_0 + E_1 \cos(\omega t)$ into the expression for polarizability and extracting the

second harmonic term gives

$$P^{2\omega} = \epsilon_0 E_1^2 \left(\frac{1}{2} \chi^{(2)} + \frac{3}{2} \chi^{(3)} E_0 \right) \cos(2\omega t) = \epsilon_0 E_1^2 \chi_{\text{eff}}^{(2)} \cos(2\omega t) \quad (1)$$

The dominant macroscopic second-order polarization element is

$$\chi^{(2)} = N\beta \langle \cos^3\theta \rangle$$

where N is the chromophore volume density, β is the dominant second-order microscopic polarizability, and $\langle \cos^3\theta \rangle$ is an order parameter that can be expressed in terms Langevin function of order 3.¹⁷ A noncentrosymmetric alignment as induced by electric field poling induces a $\chi^{(2)}$ in the polymer film. In this investigation a corona discharge is used to apply a large electric field to the polymer film to orient the nonlinear chromophore.¹⁸ The intensity of the generated second harmonic is

$$I_{2\omega} \approx Ad^2 \chi_{\text{eff}}^{(2)2} I_{\omega}^2$$

where A is a proportionality constant and d is the film thickness provided that the film is considered to be lossless and the thickness is small so that $|n_2 - n_1|d < \lambda_{2\omega}$ where n_2 and n_1 are the indices of refraction at the second harmonic wavelength $\lambda_{2\omega}$ and fundamental wavelength λ_{ω} , respectively.

The corona poling was performed in either a poling station or in an in situ cell that provides simultaneous poling and SHG monitoring. In the poling station, the substrate is placed on a temperature-controlled grounded aluminum block. Typical conditions in the poling station for 1 mm thick sodalime substrates with a corona wire suspended 1 cm above the substrate involve poling voltages in the range of 6 kV and poling currents in the range of 2 μ A. Poling is performed at an elevated voltage and temperature for at least $1/2$ h and then gradually cooled to room temperature while the poling field is still applied. Use of a temperature-controlled in situ poling cell permits more control on the optimization of the poling process. For such measurements the glass substrate has an indium tin oxide coating on the opposite surface on which the polymer is deposited. A high-voltage current-controlled power supply is connected to a thin tungsten wire (40 μ m diameter) held at 1 cm above the polymer film and the ITO-coated side is grounded. A thermocouple is placed on the edge of surface of the polymer film and it is electrically isolated from the discharge (e.g., by wrapping it in Teflon tape) to avoid current flow from the corona discharge to the temperature controller through the thermocouple. To make sure that the current from the corona wire is conducted through the polymer film and substrate to ground, it is measured between the power supply and the corona wire and between the conducting plane in contact with the glass substrate and ground. A measurement of the temperature distribution on the sample surface is used to account for the difference, in the in situ SHG measurements, between the region where the second harmonic measurement is performed and the edge of the sample where the temperature is measured. The lock-in amplifier, temperature controller, and one of the picoamperimeters were interfaced to a computer to record the second harmonic signal, temperature, and poling current as a function of time. All films were maintained at elevated voltage and temperature for at least 30 min and then cooled to room temperature while keeping the poling voltage constant. After corona poling, a significant surface charge remains on the polymer surface that must be removed to obtain an accurate assessment of the second harmonic signal produced by solely by the orientation of the nonlinear chromophores. As can be seen in eq 1 the presence of a static electric field will enhance the second harmonic intensity through the third-order optical nonlinearity $\chi^{(3)}$. This contribution is called the electric field enhanced second harmonic (EFISH). If, for example, after poling the change in the orientation of the nonlinear chromophore is of interest, since the surface charge will also slowly decay, the presence

of an EFISH contribution will lead to erroneous conclusions. To eliminate the EFISH contribution, the surface charge is removed by immersing the samples into unpurified water for 5–10 min. To illustrate the importance of eliminating the EFISH contribution in this manner, we corona poled a **LCP1** film and performed measurements of the surface potential and second harmonic generated by the film after poling and after immersing the sample in water. The surface potential is measured with an electrostatic voltmeter that permits voltage measurements of electrostatic sources without physical contact. A film of **LCP1** (480 nm thick) cast on a 1 mm thick sodalime glass substrate was used for the experiment. Immediately after poling, the surface potential, measured over an area of 5×2 cm, was in the 165 ± 15 V range resulting in an average electric field of 344 V/ μ m. The film generated a second harmonic signal of 8.6 au. After the sample is immersed in water, the electric field is reduced to 46 V/ μ m and the second harmonic signal is reduced to 2.5 au. Given such a relatively small electric field, the assumption is made that the EFISH contribution is negligibly small, and second harmonic signal is dominated by the contribution from $\chi^{(2)}$.

Measurements of the new materials, such as **LCP1**, were done in comparison with a well-known and well-characterized NLO polymer DR1-MMA. The optimal poling conditions for the DR1-MMA films, defined as repeatable second harmonic intensity signals during and after poling measured on multiple samples prepared in similar manner, were established at ~ 100 °C with a voltage around 5.7 kV and current of about ~ 2 μ A (note that these conditions are specific to our poling configuration). The ratio of effective susceptibilities of the reference material with respect to the material under test is calculated by the equation

$$\frac{\chi_{\text{REFeff}}^{(2)}}{\chi_{\text{TESTeff}}^{(2)}} = \sqrt{\frac{P_{\text{REF}}^{2\omega} \left(\frac{P_{\text{TEST}}^{\omega} L_{\text{TEST}} \right)^2}{P_{\text{TEST}}^{2\omega} \left(\frac{P_{\text{REF}}^{\omega} L_{\text{REF}} \right)^2}} \quad (2)$$

where P^{ω} is the fundamental laser power incident on the film, $P^{2\omega}$ is the second harmonic power generated by the film, and L is the thickness of a particular film.

Synthesis. 4-[(2-Hydroxyethyl)(methyl)amino]benzaldehyde (3). Into a 500 mL flask containing a magnetic stirring bar and 250 mL of dimethyl sulfoxide were added 30.0 g (0.40 mol) of 2-(methylamino)ethanol, 52.0 g (0.38 mol) of potassium carbonate, and 5 drops of tricarbonylmethylammonium chloride. The mixture was heated to 90 °C with stirring, and then 37.2 g (0.30 mol) of 4-fluorobenzaldehyde was added dropwise. The reaction was continued for 35 h at 90 °C, and after cooling the mixture was poured into 1 L of ice water with vigorous stirring. The product was extracted with dichloromethane, and the organic layer was separated, dried with magnesium sulfate, and evaporated to give a liquid that was added dropwise to cold petroleum ether with stirring. The precipitated yellow solid was collected and recrystallized from toluene twice to give light yellow fine crystals of **3**. Yield: 31 g (58%). DSC: mp 71.0 °C¹⁹ (onset 69.8 °C). ¹H NMR (CDCl₃): δ 9.71 (s, 1H, CHO), 7.65 (d, 2H, ArH), 6.77 (d, 2H, ArH), 3.83 (t, 2H, CH₂), 3.60 (t, 2H, CH₂), and 3.12 (s, 3H, NCH₃).

4-(Diethylamino)-2-[(6-hydroxyhexyl)oxy]benzaldehyde (8). Into a 250 mL flask were placed 9.66 g (0.05 mol) of 4-(diethylamino)salicylaldehyde (**7**), 13.66 g (0.10 mol) of 6-chloro-1-hexanol (**6**), and 100 mL of *N,N*-dimethylformamide (DMF) and 30 mL of toluene. Anhydrous potassium carbonate, 3.50 g (0.025 mol), was added to the solution, and the mixture was heated for 24 h while distilling out water by means of a Dean–Stark trap. After cooling, the product was isolated by extraction with ethyl acetate vs water and the organic layer was dried with magnesium sulfate and condensed by rotary evaporation. The residual liquid was chromatographed on a silica gel column (ethyl acetate/petroleum ether = 1/1), to give the product **8** as dark brown oil. Yield: 9.70 g (66%). ¹H NMR (CDCl₃): δ 7.72 (d, 1H, ArH), 6.30 (d, 1H, ArH), 6.07 (s, 1H, ArH), 4.04 (t, 2H, OCH₂), 3.67 (t, 2H, CH₂OH), 3.42 (q, 2H, NCH₂), 1.86–1.85 (m, 2H, CH₂), 1.62–1.45 (m, 4H, CH₂), and 1.22 (t, 6H, CH₃).

Ethyl 2-Cyano-2-(3,5,5-trimethyl-2-cyclohexenylidene)acetate (11). To a 500 mL flask equipped with a Dean–Stark trap and a condenser were added 27.64 g (0.2 mol) of isophorone (**10**), 22.60 g (0.20 mol) of ethyl cyanoacetate (**9**), 200 mL of benzene, 16 mL of acetic acid, and 8 g of sodium acetate. The mixture was stirred at reflux while distilling benzene for 28 h. After cooling, water was added and the mixture was transferred to a separatory funnel; the organic layer was separated, dried with magnesium sulfate, filtered, and then evaporated. The resulting viscous oil was transferred to a 100 mL one-neck flask and distilled under vacuum (bp 168–170 °C/6 Torr) to give the product **11** as a light yellow liquid. Yield: 38.6 g (83%). ¹H NMR (CDCl₃): δ 7.61 (s, 0.5H, =CH), 6.67 (s, 0.5H, =CH), 4.28–4.25 (m, 2H, CH₂CH₃), 2.90 (s, 2H, cyclic CH₂), 2.55 (s, 2H, cyclic CH₂), 2.12–1.98 (m, 3H, CH₃), 1.35 (t, 3H, CH₂CH₃), and 1.00 (d, 6H, (CH₃)₂).

2-(Ethylanilino)ethyl Bicyclo[2.2.1]hept-5-ene-2-carboxylate (15). Into a 500 mL flask were placed 66.50 g (0.40 mol) of 5-norbornene-2-carboxylic acid ethyl ester (**13**), 33.05 g (0.20 mol) of 2-(*N*-ethylanilino)ethanol (**2**), and 200 mL of toluene. Dibutyltin oxide 1.24 g (5 mmol) was added to this solution, which was heated to 160 °C while continuously removing toluene over 6 h. The residual mixture was transferred to a 250 mL flask and vacuum distilled (bp 174–175 °C/0.4 Torr) to give the product **15** as a viscous liquid. Yield: 40.0 g (70%). ¹H NMR (CDCl₃): δ 7.24 (d, 2H, ArH), 6.73 (broad s, 3H, ArH), 6.20–5.90 (m, 2H, CH=CH), 4.19 (t, 2H, OCH₂), 3.57–3.38 (m, 4H, CH₂NCH₂), 3.19–1.26 (m, 7H, norbornene-7H), and 1.18 (t, 3H, CH₃).

2-(Ethyl-4-formylanilino)ethyl Bicyclo[2.2.1]hept-5-ene-2-carboxylate (16). Into a flask containing 100 mL of DMF was added 30.7 g (0.20 mol) of phosphorus oxychloride (POCl₃) dropwise at 0 °C, and then compound **15** (28.5 g, 0.10 mol) dissolved in 50 mL of DMF was added slowly using a dropping funnel at room temperature. The reaction was stirred at room temperature for 3 h, and then the mixture was warmed at 90 °C for 1 h. After cooling, the mixture was poured slowly into ice water with stirring, and aqueous NaOH solution was added slowly until pH 6 was reached. The mixture was then extracted with ethyl acetate and the product was purified by column chromatography (ethyl acetate/petroleum ether = 1/2) to give the product **16** as a viscous yellow liquid. Yield: 17.5 g (56%). ¹H NMR (CDCl₃): δ 9.75 (s, 1H, CHO), 7.73 (d, 2H, ArH), 6.80 (d, 2H, ArH), 6.18–5.86 (m, 2H, CH=CH), 4.22 (t, 2H, OCH₂), 3.67–3.47 (m, 4H, CH₂NCH₂), 3.19–1.38 (m, 7H, norbornene-H), and 1.23 (t, 3H, CH₃).

2-[4-Formyl(methyl)anilino]ethyl Bicyclo[2.2.1]hept-5-ene-2-carboxylate (17). Into a 100 mL flask were added 4.99 g (0.03 mol) of 5-norbornene-2-carboxylic acid ethyl ester (**13**), 3.58 g (0.02 mol) of compound **3**, 50 mL of toluene, and dibutyltin oxide (0.124 g (0.5 mmol)). The solution was heated at 160 °C while toluene was slowly removed over 5 h using a Dean–Stark trap. After concentration, the remaining liquid was purified by column chromatography (ethyl acetate/petroleum ether = 1/3), yielding **17** as a yellow viscous oil. The yield was 4.90 g (82%). ¹H NMR (CDCl₃): δ 9.75 (s, 1H, CHO), 7.74 (d, 2H, ArH), 6.78 (d, 2H, ArH), 6.16–5.81 (m, 2H, CH=CH), 4.23 (t, 2H, OCH₂), 3.68 (t, 2H, NCH₂), 3.10 (s, 3H, NCH₃), and 2.89–1.22 (m, 7H, norbornene-H).

Synthesis of NLO Chromophores. 4-((E)-2-[4-[Ethyl-(2-hydroxyethyl)amino]phenyl]-1-diazenyl)benzotrile (C2). Into a 100 mL flat-bottom flask were added 20 mL of concentrated hydrochloric acid and 2.36 g (0.02 mol) of 4-aminobenzotrile (**1**) with stirring. In another test tube, 1.38 g (0.02 mol) of sodium nitrite was dissolved in 2 mL of water, and this aqueous solution was then added dropwise into the prepared **1** solution at 0 °C and stirred for 2 h. To this yellow diazonium salt solution, the 2-(*N*-ethylanilino)ethanol solution (3.30 g, 0.02 mol) diluted with 10 mL of hydrochloric acid was added slowly at 0 °C for 1 h and stirred at room temperature for 20 h more. The red product mixture was poured into cold water and sodium bicarbonate was added slowly to neutralize the solution. The fine orange precipitate was filtered and recrystallized from acetic acid, to give **C2** as orange crystals. Yield: 4.20 g (71%). UV (CH₃CN): λ_{max} 459 nm. DSC (5 °C/

min): mp 144.3 °C, onset 142.4 °C. ¹H NMR (CDCl₃): δ 7.95–7.90 (m, 4H, ArH), 7.75 (d, 2H, ArH), 6.87 (d, 2H, ArH), 3.91 (t, 2H, OCH₂), 3.69–3.55 (m, 4H, CH₂NCH₂), and 1.27 (t, 3H, CH₃).

2-Methyl-4-[(E)-2-(4-nitrophenyl)-1-ethenyl]anilino-1-ethanol (C3). Compound **3** (8.96 g, 0.05 mol), 18.11 g (0.1 mol) of 4-nitrophenylacetic acid (**4**) and 30 mL of DMF were placed into a 100 mL flask. After the reaction was warmed to 40 °C, piperidine (10 mL) was added dropwise, and the mixture was heated at 100 °C for 10 h. The cooled reaction mixture was poured into water to precipitate the product that was isolated by suction filtration and recrystallized from ethanol, giving **C3** as red crystals. Yield: 3.73 g (25%). UV (CH₃CN): λ_{max} 437 nm. DSC (5 °C/min): mp 184.7 °C, onset 179.0 °C. ¹H NMR (CDCl₃): δ 8.18 (d, 2H, ArH), 7.56 (d, 2H, ArH), 7.45 (d, 2H, ArH), 7.20 (d, 1H, CH=), 6.94 (d, 1H, CH=), 6.81 (d, 2H, ArH), 3.86 (t, 2H, OCH₂), 3.56 (t, 2H, NCH₂), and 3.06 (s, 3H, NCH₃).

2-[3-((E)-2-[4-(2-Hydroxyethyl)(methyl)amino]phenyl)-1-ethenyl]-5,5-dimethyl-2-cyclohexenylidene]malononitrile (C4). To a 250 mL flask with a magnetic stirring bar and a condenser were added 3.58 g (0.02 mol) of compound **3**, 50 mL of 1-propanol, 3.73 g (0.02 mol) of 1,5,5-trimethylcyclohex-(2-enylidene)-malononitrile (**5**) and 10 drops of piperidine, and then the solution was stirred at 100 °C for 24 h. After TLC indicated that all of **3** was consumed, the reaction mixture was cooled to room temperature, was concentrated by rotary evaporation, and then was poured into petroleum ether with vigorous stirring. The precipitated material was collected and recrystallized from toluene to give **C4** as fine red crystals. Yield: 4.90 g (65%). UV (CH₃CN): λ_{max} 501 nm. DSC (5 °C/min): mp 151.7 (onset 146.3) and 158.8 °C. ¹H NMR (THF-*d*₆): δ 7.44 (d, 2H, ArH), 7.13 (d, 1H, CH=), 6.97 (d, 1H, =CH), 6.74–6.72 (m, 3H, ArH), 3.67 (d, 2H, OCH₂), 3.50 (t, 2H, NCH₂), 3.06 (s, 3H, NCH₃), 2.57 (s, 2H, cyclic CH₂), 2.51 (s, 2H, cyclic CH₂), and 1.05 (s, 6H, (CH₃)₂).

6-{5-(Diethylamino)-2-[(E)-2-(4-nitrophenyl)-1-ethenyl]-phenoxy}-1-hexanol (C5). Compound **8** (5.87 g, 0.02 mol) and 4-nitrophenylacetic acid (7.24 g, 0.04 mol) were placed in a 100 mL flask and dissolved in 10 mL of DMF at 40 °C. Piperidine (4 mL) was added dropwise into the solution, and the mixture was heated at 100 °C for 10 h and after cooling the reaction mixture was poured into water to precipitate the product. The crude product was recrystallized from ethanol, giving **C5** as red crystals. Yield: 2.10 g (25%). UV (CH₃CN): λ_{max} 457 nm. DSC (5 °C/min): mp 88.7 °C, onset 85.7 °C. ¹H NMR (CDCl₃): δ 8.15 (d, 2H, ArH), 7.59–7.46 (m, 3H, ArH), 7.35 (d, 1H, CH=), 6.99 (d, 1H, CH=), 6.31 (d, 1H, ArH), 6.16 (s, 1H, ArH), 4.05 (t, 2H, OCH₂), 3.67 (t, 2H, CH₂OH), 3.39 (q, 4H, NCH₂), 1.92 (t, 2H, CH₂), 1.66–1.48 (m, 6H, CH₂), and 1.21 (t, 6H, CH₃).

Ethyl-2-cyano-2-(3-[(E)-2-[4-(dimethylamino)phenyl]-1-ethenyl]-5,5-dimethyl-2-cyclohexenylidene)acetate (C6). Into a 100 mL flask were added 2.98 g (0.02 mol) of 4-*N,N*-dimethylaminobenzaldehyde (**12**), 4.66 g (0.02 mol) of compound **11**, 40 mL of 1-propanol, and 10 drops of piperidine. The solution was heated at 120 °C with stirring for 25 h, the mixture was stored in a refrigerator overnight, and the crystals of **C6** were collected by filtration, washed with petroleum ether, and dried. Yield: 2.9 g (40%). UV (CH₃CN): λ_{max} 470 nm. DSC (5 °C/min): mp 189.5 °C, onset 184.7 °C. ¹H NMR (CDCl₃): δ 7.41 (d, 2H, ArH), 6.97–6.77 (m, 4H, CH=CH and ArH), 4.27 (q, 2H, CH₂), 3.04 (s, 3H, NCH₃), 2.98 (s, 2H, cyclic CH₂), 2.40 (s, 2H, cyclic 2H), 1.37 (t, 3H, CH₂CH₃), and 1.04 (s, 6H, (CH₃)₂).

Synthesis of NLO Norbornene Monomers M1–M9. See Supporting Information for these syntheses.

Synthesis of NLO Poly(norbornenes). Preparation of Polymerization Catalyst Solutions. Preparation of catalyst solution A for polymerization of **HP**, **BP**a through **BPI**, and **CP1** through **CP9** was performed on a 2 mmol scale as follows: In an oxygen- and moisture-free glovebox, 0.098 g (0.2 mmol) of the nickel catalyst and 10 mL of toluene were placed in a 10 mL serum bottle to give a dark brown solution. The bottle was tightly sealed. Preparation of catalyst solution B was performed for 20–40 mmol scale polymerization of **LCPI**

Table 1. Results of the Transesterification Study Using Ti or Sn Catalysts

no.	13/DR1 ratio	reaction condition ^a			convn ^b (%)	yield (%) ^c
		catalyst	cat. concn (mol %)	time (h)		
T1	1/1	Ti	1	4	>50	45
T2	1/1	Ti	1	24	>50	
T3	1/1	Ti	5	4	>70	
T4	2/1	Ti	5	4	>80	
T5	1/1	Sn	5	4	>70	65
T6	2/1	Sn	5	4	>90	71
T7	3/1	Sn	5	4	>95	78

^a NB: 0.01 mol; toluene 50 mL; N₂; reflux; Ti, titanium isopropoxide; Sn, dibutyltin oxide. ^b Checked by LC. ^c Purified by chromatography, followed by recrystallization.

Table 2. Physical Properties and Exo/Endo Ratios of Norbornene Functionalized Monomers Used in This Study

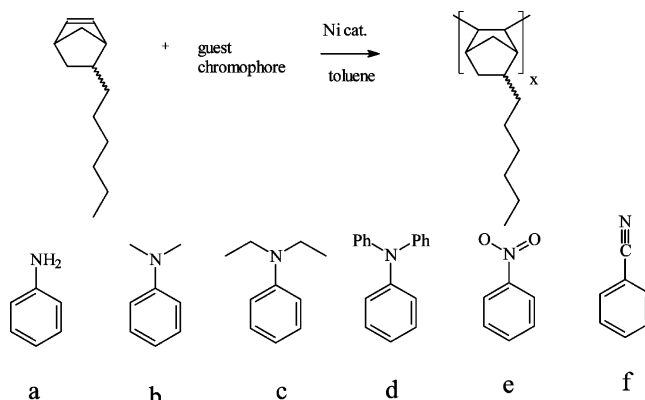
norbornene monomer	MW	mp ^a (°C)	bp (°C/Torr)	λ _{max} ^b (nm)	exo ^c (%)	endo ^c (%)
13	166.21		78/10		39.9	60.1
14	124.18		103/20		21.0	79.0
15	285.38		175/0.4		21.0	79.0
16	313.39				21.5	78.5
17	299.36				20.5	79.5
18	178.31		116/20		28.7	71.3
M1	434.49	76.8		478	40.7	59.3
M2	414.50	94.1		448	36.0	64.0
M3	418.49	118.9		432	38.9	61.1
M4	467.61	121.2		493	20.0	80.0
M5	532.68	58.4		458		<i>d</i>
M6	442.60	159.8		472	20.6	79.4
M7	432.51	94.4		435	32.5	67.5
M8	408.49	94.0		420	33.8	66.2
M9	514.66			472	37.1	62.9

^a Peak points measured by DSC. ^b Absorption maxima measured by UV-vis spectroscopy in acetonitrile. ^c Calculated values from ¹H NMR spectra. ^d The ratio could not be calculated due to peak overlap.

through LCP4 as follows: In an oxygen- and moisture-free glovebox, 0.98 g (2.0 mmol) of the nickel catalyst and 50 mL of toluene was placed in a 100 mL serum bottle and then sealed tightly.

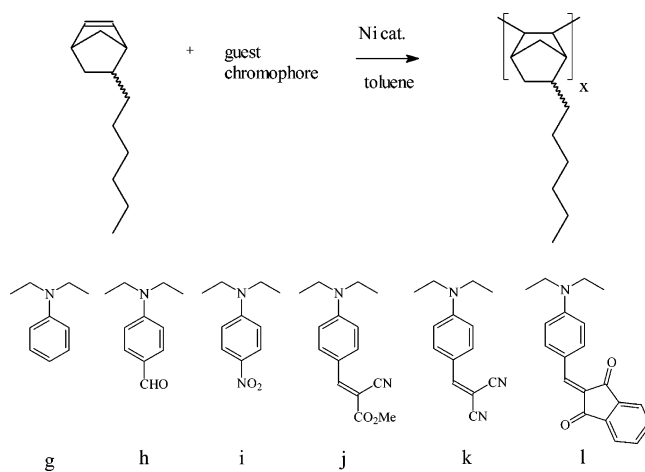
Homopolymerization. Into a dried 20 mL serum bottle were added 0.357 g (2 mmol) of 5-hexyl-2-norbornene (or 5-hexyl norbornene) (**18**), 5 mL of anhydrous toluene, and a magnetic stirring bar. The bottle was sealed, and the solution was deaerated with a stream of nitrogen introduced and removed with syringe needles. Then the catalyst solution A (1 mL) was injected all at once with vigorous stirring. The solution became viscous within 2 min and after 24 h at room temperature the viscous polymer solution was diluted with toluene and about 1 g of ion-exchange resin (Amberlite IRC 718, to remove the catalyst) was added and the solution stirred for 5 h. After vacuum filtration, the filtrate was added dropwise into acetone with vigorous stirring. The precipitated white pulplike poly(hexylnorbornene) was collected by suction filtration and dried overnight in an oven at 80 °C. Yield: 0.349 g (98%). The weight-average molecular weight (*M_w*) was determined to be 1 731 000.

Blend Polymerization. A representative example of a blend polymerization that was run to evaluate the compatibility of functional groups with the Ni catalyst follows. Into a dried serum bottle were placed 0.357 g (2.0 mmol) of 5-hexyl-2-norbornene (**18**) and 0.0606 g (0.5 mmol) of *N,N*-dimethylaniline followed by 5 mL of anhydrous toluene and a magnetic stirring bar. The bottle was capped, sealed, and deaerated with argon for 20 min. The catalyst solution A (1 mL) was injected with a syringe into the polymerization bottle with vigorous stirring. After 24 h at room temperature, about 1 g of ion-exchange resin (Amberlite IRC 718) was added into the

Table 3. Results of Blend Polymerization of Hexylnorbornene in the Presence of 20 mol % of a Variety of Nitrogen-Containing Compounds^a

no.	guest compound	yield ^b (%)	<i>M_w</i> (×10 ³)	<i>M_n</i> (×10 ³)	<i>M_w/M_n</i> ^b
HP		98	1731	346	5.01
BP _a	a	0			
BP _b	b	94	472	77	6.11
BP _c	c	90	971	131	7.41
BP _d	d	98	1371	349	3.93
BP _e	e	97	1046	208	5.04
BP _f	f	0			

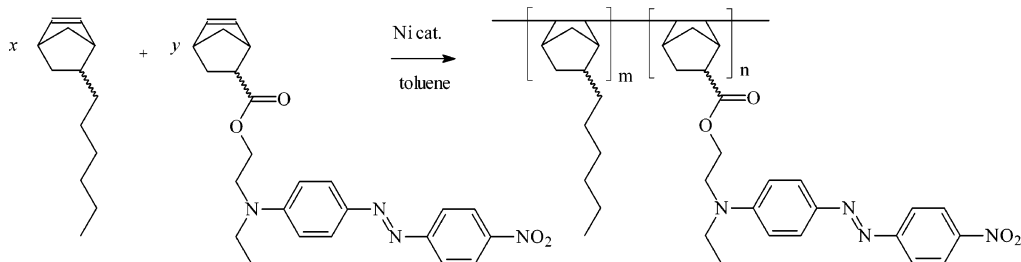
^a Monomer: 2 mmol. Guest: 0.5 mmol. Ni catalyst concentration: 0.02 mmol. Solvent: toluene, 6 mL. Temperature: room temperature. Time: 24 h. ^b After one precipitation

Table 4. Results of Blend Polymerization Results in the Presence of 20 mol % *N,N*-Diethylaniline Derivatives^a

no.	guest compound	concn (mmol)	yield ^b (%)	<i>M_w</i> (×10 ³)	<i>M_n</i> (×10 ³)	<i>M_w/M_n</i> ^b
HP			98	1731	346	5.01
BP _g	g	0.5	90	971	131	7.41
BP _h	h	0.5	87	81	28	2.89
BP _i	i	0.5	92	276	86	3.12
BP _j	j	0.5	0			
BP _k	k	0.5	0			
BP _l	l	0.5	92	359	91	3.96

^a Ni catalyst concentration: 0.02 mmol. Solvent: toluene, 6 mL. Temperature: room temperature. Time: 24 h. ^b After two precipitations.

polymerization bottle and stirred for 5 h. After filtration, the polymer solution was added dropwise to acetone while stirring. The precipitated white poly(norbornene) was collected by filtration and dried overnight in oven at 80 °C. Yield: 0.335 g (94%). The weight-average molecular weight (*M_w*) was determined to be 472 000. The other blend polymerizations (BP_a through BP_l in Table 3 and Table 4) were carried out using

Table 5. NLO Copolymerization Results of CP1 from M1^a

no.	<i>x/y</i>	18 (mmol)	M1 (mmol)	toluene (mL)	catalyst (mmol)	yield ^b (%)	<i>m/r</i> ^c (%/%)	<i>M_w</i> (×10 ³)	<i>M_n</i> (×10 ³)	<i>M_w/M_n</i>
CP1a	80/20	1.6	0.4	8	0.02	70		99	47	2.09
CP1b	80/20	1.6	0.4	6	0.02	76		125	56	2.22
CP1c	80/20	1.6	0.4	4	0.02	70		107	49	2.18
CP1d	80/20	1.6	0.4	2	0.02	37		53	25	2.16
CP1e	80/20	1.6	0.4	6	0.01	74		128	50	2.58
CP1f	80/20	1.6	0.4	6	0.02	76		125	56	2.22
CP1g	80/20	1.6	0.4	6	0.03	65		95	38	2.50
CP1h	80/20	1.6	0.4	6	0.04	59		94	43	2.18
HP	100/0	2.0	0.0	6	0.02	98	100.0/0.0	1731	346	5.01
CP1i	80/20	1.6	0.4	6	0.02	76	83.3/16.7	125	56	2.22
CP1j	70/30	1.4	0.6	6	0.02	65	76.5/23.5	84	44	1.90
CP1k	60/40	1.2	0.8	6	0.02	36	69.9/30.1	56	32	1.73
CP1l ^d	50/50	1.0	1.0	6	0.02	19	64.3/35.7	69	33	2.12

^a Polymerization temperature: room temperature. Polymerization time: 24 h. ^b After two precipitations. ^c Measured by ¹H NMR spectrometry. ^d Polymerization time: 3 days.

the same procedure as described above except other additives were substituted for the *N,N*-dimethylaniline.

Copolymerization. Several representative examples of copolymerization follow in which more than one norbornene monomer was used. All of the initial copolymerizations described here were run using a total of 2 mmol of monomers.

LCP1(8/2). Into a dried 20 mL serum bottle were placed 0.285 g (1.6 mmol) of 5-hexyl-2-norbornene (**18**), 0.174 g (0.4 mmol) of **M1**, 5 mL of anhydrous toluene, and a magnetic stirring bar. This bottle was sealed and deaerated for 20 min using nitrogen. The catalyst solution A (1 mL) was injected all at once into the polymerization bottle with vigorous stirring. After 24 h at room temperature, the viscous polymer solution was diluted with toluene, about 1 g of ion-exchange resin (Amberlite IRC 718) was added to remove Ni catalyst, and the mixture was stirred for 5 h. After vacuum filtration, the dark red polymer solution was added dropwise into acetone while stirring. The precipitated copolymer was dissolved again in toluene and this polymer solution was precipitated once more in acetone. The red powder was collected by filtration, washed thoroughly with acetone until the red color in the acetone wash could not be detected, and dried overnight in an oven at 80 °C. Yield: 0.41 g (73%). The weight-average molecular weight (*M_w*) was determined to be 125 000.

The other 2 mmol-scale copolymerizations (CP1a through CP1l in Table 5 and CP1(7/3) through CP4(8/2) in Table 6) were carried out using this same general procedure. After initial screening on a 2 mmol scale some of the polymerizations were scaled up to a preparative level of LCP (20–40 mmol scale).

LCP1(8/2). Into a dried 200 mL serum bottle were placed 5.706 g (32 mmol) of 5-hexyl-2-norbornene (**18**) and 3.476 g (8 mmol) of **M1**, 100 mL of anhydrous toluene, and a magnetic stirring bar. This bottle was sealed and deaerated for 30 min with argon. The catalyst solution B (10 mL) was injected all at once into a polymerization bottle with vigorous stirring. After polymerization at room temperature for 24 h, the viscous polymer solution was diluted with toluene and about 20 g of ion-exchange resin (Amberlite IRC 718) was added to remove catalyst and the mixture was stirred for 5 h. After vacuum filtration, the dark red polymer solution was added dropwise to acetone while stirring. The precipitated copolymer was dissolved again in toluene, and this polymer solution was precipitated again in acetone. The red powder was collected by filtration and dried overnight in an oven at 80 °C. Yield:

Table 6. Results of Copolymerization of NLO Functionalized Monomers with Hexylnorbornene (Monomer: 2 mmol Scale)^a

no.	<i>R</i>	<i>x/y</i>	yield (%)	<i>M_w</i> (×10 ³)	<i>M_n</i> (×10 ³)	<i>M_w/M_n</i>
CP1(8/2)	1	80/20	76	125	56	2.22
CP1(7/3)	1	70/30	65	84	44	1.90
CP2(8/2)	2	80/20	82	270	69	3.90
CP2(7/3)	2	70/30	74	186	46	4.07
CP3(8/2)	3	80/20	76	328	69	4.73
CP3(7/3)	3	70/30	69	253	60	4.21
CP4(8/2)	4	80/20	78	386	101	3.30
CP5	5	95/5	0			
CP6	6	95/5	0			
CP7	7	95/5	0			
CP8	8	95/5	0			
CP9	9	95/5	0			

^a *x* + *y* = 2 mmol, polymerization temperature: RT, polymerization time: 24 h.

8.16 g (89%). The weight-average molecular weight (*M_w*) was determined to be 123 000.

LCP2(7/3). Into a dried 100 mL serum bottle were placed 2.496 g (14 mmol) of 2-hexyl-5-norbornene (**18**) and 2.511 g (6 mmol) of **M3**, 50 mL of anhydrous toluene, and a magnetic stirring bar. This bottle was sealed and deaerated for 30 min with nitrogen. The catalyst solution B (5 mL) was injected all at once into a polymerization bottle with vigorous stirring. After polymerization at room temperature for 24 h, the viscous polymer solution was diluted with toluene and about 10 g of ion-exchange resin (Amberlite IRC 718) was added to remove catalyst and the mixture was stirred for 5 h. After vacuum filtration, the dark red polymer solution was added dropwise to acetone while stirring. The precipitated red powder was collected by filtration and dried overnight in oven at 80 °C. Yield: 4.33 g (87%). The weight-average molecular weight (*M_w*) was determined to be 185 000.

Results and Discussion

Synthesis of Chromophores. The synthetic routes of all the NLO chromophores involved in this study are shown in Figure 2 either in part a or part b. These chromophores are all alcohol or ester functionalized so as to eventually attach to a complementary ester or

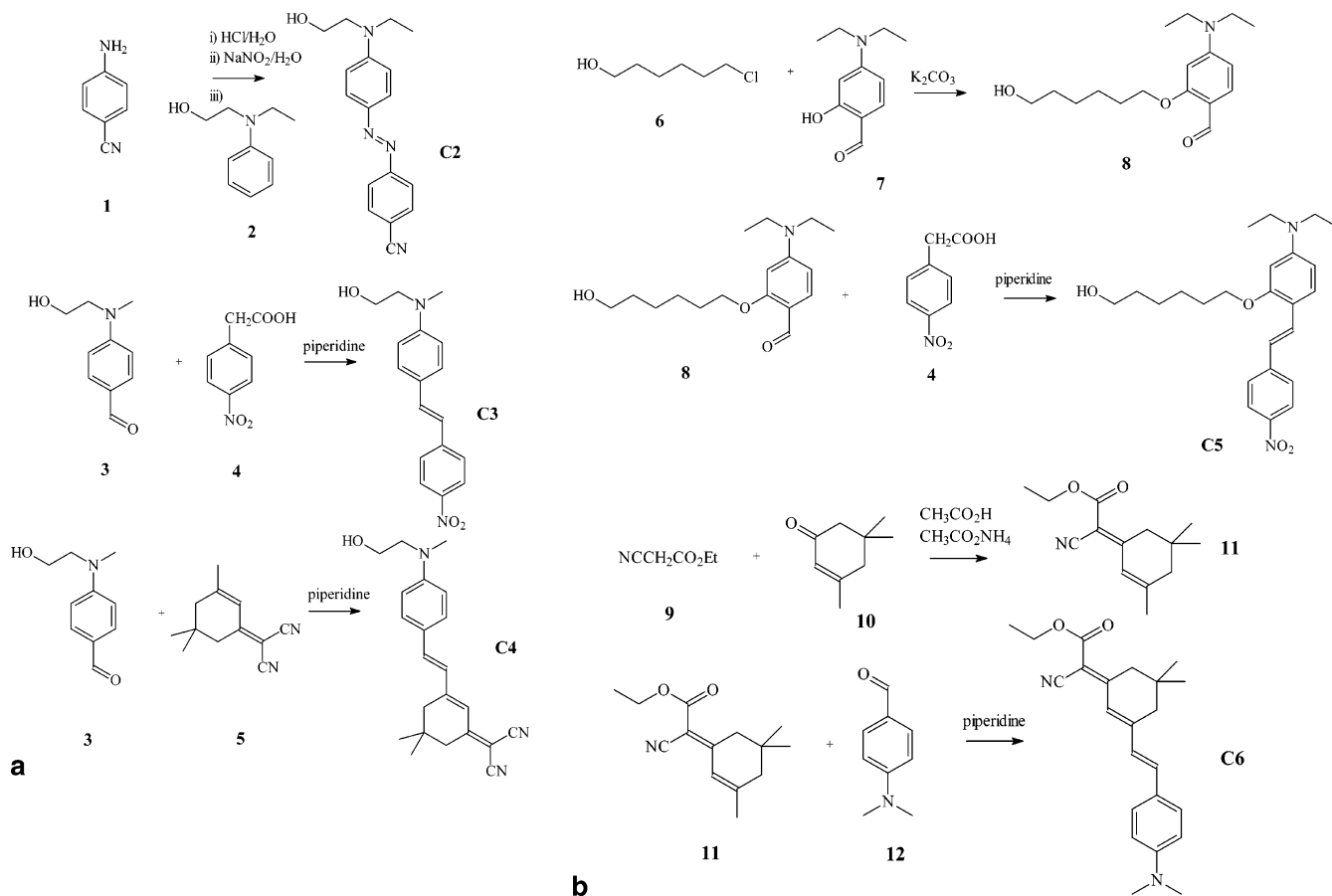


Figure 2. (a) Synthesis of the NLO chromophores that contain a link through the donor amine group. (b) Synthesis of the NLO chromophores that contain a link through a site other than the donor amine group.

alcohol-functionalized norbornene by transesterification chemistry. Chromophore **C1** (Disperse Red 1, or DR1) was commercially available while chromophores **C2**–**C6** were synthesized by standard diazonium coupling or by Knoevenagel condensation. The NLO chromophores in this study contain an azobenzene, stilbene, or isophorone-derived π -conjugated bridge, a *N,N*-dimethylaniline or a *N,N*-diethylaniline unit as an electron donor and a nitro, cyano, dicyanovinyl, or cyano-estervinyl group as an electron acceptor. These types of chromophores are well-known, are well characterized, and have been employed in numerous other nonlinear optical polymers.^{20,21}

The starting material **3** was synthesized by a reaction of *N*-methylaminoethanol with an excess of 4-fluorobenzaldehyde in the presence of a phase transfer agent at 90 °C. At higher temperature, byproducts increased significantly, which were found to be due to aromatic nucleophilic substitution of both amine and alcohol. Compound **8** was synthesized by a condensation reaction of **6** with **7** using potassium carbonate as a base, and compound **11** was prepared by a condensation reaction from isophorone.

Azobenzene **C2** was prepared by a general diazonium coupling procedure.²² Both **C3** and **C5** were synthesized by Knoevenagel condensation using **4**, the yields of which were low despite use of excess **4** (which tends to decarboxylate to 4-nitrotoluene). Chromophore **C5** having both a longer aliphatic group and different site of attachment than **C3** was synthesized so that the influence of a longer spacer group on poling could be evaluated. The chemical structures of all these chromophores were confirmed by ¹H NMR spectroscopy and

they all showed one sharp endothermic melting peak except for **C4** that exhibited two peaks due to two crystal forms.

Synthesis of Functionalized NLO Monomers. Details regarding the synthesis of the NLO monomers (**M1**–**M9**) are given in the Supporting Information. The chromophore-functionalized norbornene monomers were synthesized by a transesterification reaction between norbornene ethyl ester (**13**) with a hydroxy-substituted chromophore (**C1**–**C5**) to give **M1**–**M5** or between norbornenemethanol (**14**) with the ester-substituted chromophore **C6** to give **M6**. These reaction schemes are depicted in Figure 3 parts a and b. Since both titanium isopropoxide and dibutyltin oxide are well-known catalysts for transesterifications, as in the case of the synthesis of poly(ethylene terephthalate), we adopted these two catalysts for the synthesis of the norbornene-functionalized monomers. To determine the optimum transesterification conditions, the preparation of **M1** monomer by reaction of **13** with **C1** (DR1) under various reaction conditions was examined and the results are summarized in Table 1. Both titanium isopropoxide and dibutyltin oxide were useful for transesterifications, but the tin catalyst usually gave a little higher conversion (compare **T4** with **T6**). Because scrupulously anhydrous reaction conditions were not used in our experiments the more moisture-sensitive titanium isopropoxide was less effective. The dibutyltin oxide was preferable because it is not as sensitive to moisture or oxygen. As the **13/C1** ratio was increased to 3/1 (**T7**), the yield increased. After a prolonged exchange reaction time over 24 h, some byproducts due to destruction of the chromophore began to accumulate.

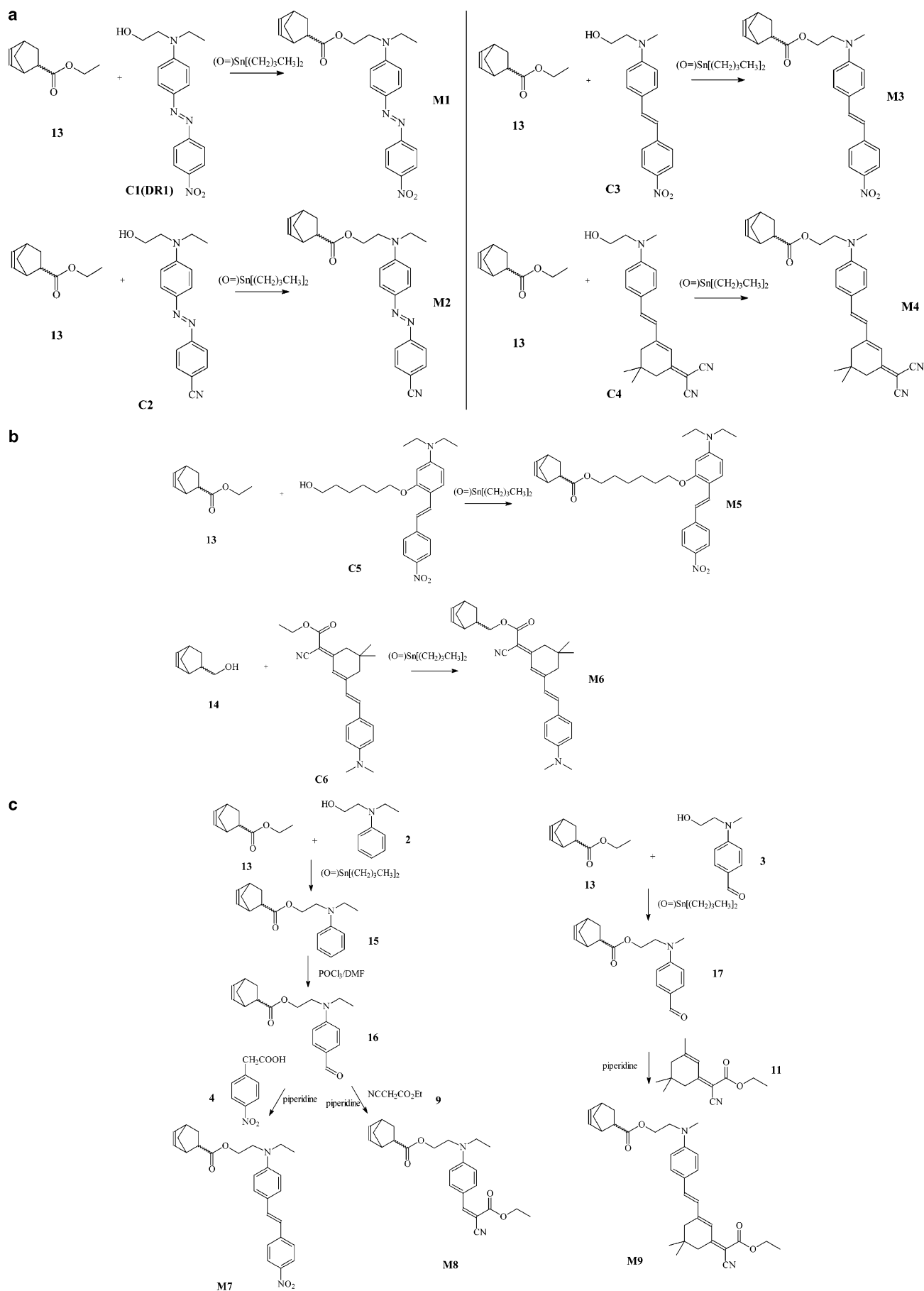


Figure 3. (a) Synthesis of NLO norbornene monomers by transesterification via a link through the donor amine group. (b) Synthesis of NLO norbornene monomers by transesterification via a link through a site other than the donor amine group. (c) Synthesis of NLO norbornene monomers by transesterification and subsequent Knoevenagel condensation.

Using reaction conditions (**T7**) involving a feed ratio of $\mathbf{13}/\mathbf{C1} = 3/1$, a catalyst concentration of 5 mol % and a reflux temperature for 4 h, the **M1** monomer could be obtained in a 78% yield after purification by silica gel chromatography. The excess of norbornene ester starting compound could be easily removed during the chromatography.

As a secondary structure modification, some chromophores with a diethylamine donor group instead of a dimethylamine donor were also prepared. There are two reasons for this change: first, the ethyl-substituted materials are slightly more nonlinear and, second, the ethyl-substituted compounds are more thermally stable.²³ We attempted to synthesize 4-[(2-hydroxyethyl)(ethyl)amino]benzaldehyde by a reaction of 2-(ethylamino)ethanol with 4-fluorobenzaldehyde analogous to the synthesis of **3**, but the desired product was obtained in poor yield due to the steric effect (ethyl vs methyl) in the aromatic nucleophilic substitution reaction. Therefore, the monomers **M7** and **M8** containing the *N*-ethyl group found in **16** were synthesized instead by a route involving first transesterification between **13** and **2** to give **15** followed by post-formylation reaction to give **16** and finally the Knoevenagel reaction with **4** and **9** producing **M7** and **M8** respectively (Figure 3c). In the Vilsmeier–Haack formylation reaction of **15**, it was fortunate that the norbornene ester acted as a good protecting group.

All the chemical structures of the norbornene containing monomers could be fully characterized by ¹H NMR spectroscopy. The norbornene ethyl ester **13**, synthesized by Diels–Alder reaction, contained *exo* and *endo* isomers, so of course the **M1** monomer also contains two isomers. Figure 4a shows the ¹H NMR spectra of the isomer mixture (the *exo*, and *endo* isomers of **M1** monomer, respectively). Because the *exo* isomer moved slightly faster than *endo* isomer on silica gel chromatography (toluene), we could separate the two red spots on preparative TLC plates for NMR analysis. All the hydrogens in structure **M1** were easily assigned in the ¹H NMR spectrum. The spectra of the *exo* and *endo* isomers differ most around 6 ppm corresponding CH=CH in the norbornene unit. The hydrogens in the 1- and 2-positions of the *exo*-norbornene (Figure 4a) had two doublets of doublets due to coupling with the adjacent two hydrogens. The hydrogens on positions 1 and 2 in the *endo*-norbornene unit had also two doublet–doublets, but with a larger coupling constant than those of the *exo* isomer.²⁴ Figure 4b shows the NMR spectra of the two isomers expanded around 6 ppm.

All the monomers (**M1**–**M9**) synthesized in this study were a mixture of *exo* and *endo* isomers. This composition of the norbornene ethyl ester starting material (**13**) is 39.9% *exo* and 60.1% *endo* by NMR. From the integral of the isomer mixtures in Figure 4b the isomer content was calculated to be 40.7% *exo* and 59.3% *endo*. In Table 2 the *exo/endo* ratio of these norbornene monomers are tabulated as well as melting points, boiling points, and maximum absorption wavelengths (λ_{\max}). The isomer ratio of **M5** could not be calculated because the CH=CH peaks overlapped with the aromatic peaks, but it can be assumed that the ratio is not much different than in their precursors.

Except for **M9** all of the NLO monomers were obtained as crystals or solids although they were mixtures of *exo/endo* isomers. In some cases, such as for **M4** and **M5**, the monomers took a long time to solidify. The

melting points of all solid monomers were determined by DSC and all these samples showed one sharp endothermic melting peak despite their isomeric composition.

Homopolymerization. We selected the norbornene derivative 5-hexyl-2-norbornene (**18**) to make the homopolymer (**HP**) and also as a comonomer, because the *n*-hexyl functional group is inert to the catalyst and also because it provides some extra solubility to any polymers that contain it. First of all, we carried out the homopolymerization of hexylnorbornene **18** (2 mmol) with (η^6 -toluene)Ni(C₆F₅)₂ (0.02 mmol, 1 mL of catalyst solution A) in an inert atmosphere. After isolation, the weight-average and number-average molecular weight (M_w and M_n) for this homopolymer (**HP**) as determined by GPC were as high as 1 731 000 and 346 000, respectively. The glass transition temperature could not be detected by DSC, but instead the T_g was determined to be about 240 °C by dynamic mechanical analysis (DMA).

Blend Polymerization. To determine the tolerance of the nickel catalyst for various functional groups, we attempted the homopolymerization of hexylnorbornene monomer (**18**) in the presence of a variety of nitrogen-containing guest compounds since most NLO chromophores consist of nitrogen atom(s) at differing levels of oxidation in either or both of the electron-donor and electron-acceptor functional groups. The concentration of each simple functionalized guest (see Table 3, **a**–**f**) was 20 mol % relative to hexylnorbornene. This functional tolerance test of (η^6 -toluene)Ni(C₆F₅)₂ is intended to provide some guidance in defining and designing norbornene functionalized NLO monomers that are compatible with the nickel system. The M_w , M_n , and polydispersities (M_w/M_n) of the poly(hexylnorbornene)s obtained in the presence of these additives are also provided in Table 3.

As a first obvious result it is clear that the polymerizations attempted in the presence of aniline (**a**) or benzonitrile (**f**) were unsuccessful. Both the primary amine and cyano groups stop the polymerization. The influence of the cyano group was particularly troublesome as it is a common structure acceptor group feature of many (and especially some of the most nonlinear) of NLO chromophores.²⁵ It is entirely possible that the cyano and amino groups render the catalyst inactive by competing with the olefin for an open coordination site on the metal. Stable complexes of the Ni(C₅F₆)₂ fragment and its palladium analogue coordinated with benzonitrile and benzylamine have been reported.²⁶ The result with aniline itself is not so troublesome because most NLO chromophores have fully substituted amines as donors and the catalyst tolerated these amines. More specifically, the polymerization in the presence of *N,N*-disubstituted aniline guests (**b**, **c**, and **d**) yielded polymers at comparable yields but with lower M_w 's than a blank polymerization without guest compound. Considering the highest M_w of **BPd** among **BPb**–**BPd**, we note that the most-hindered aniline moiety, such as **d**, was preferable in nickel-initiated polymerization. These results implied that the nickel compound easily formed a complex with a primary amine in preference to forming a reactive complex with the alkene functionality of the monomer. Triphenylamine does not appear to affect the polymerization very much since the M_w of the homopolymer is similar to the polymerization without a guest compound. This may be due to a combination of the steric hindrance and/or the reduced basicity of

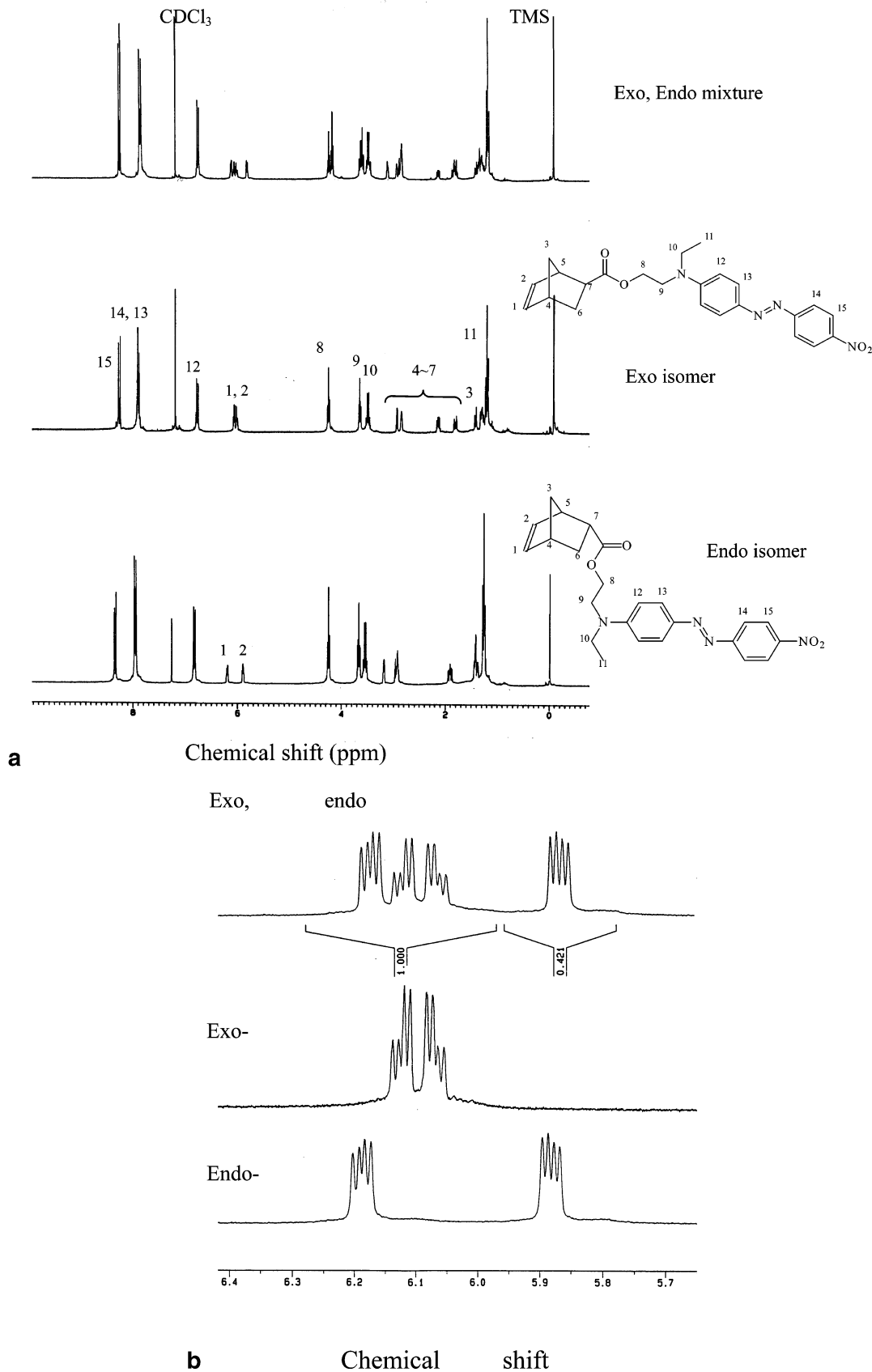


Figure 4. (a) ¹H NMR (300 MHz) spectra of the **M1** monomer stereoisomer mixture and the individual *endo* and *exo* components. (b) Expanded ¹H NMR (300 MHz) spectra of the olefinic region of the **M1** monomer mixture and of the individual pure stereoisomers.

this amine that results in weaker coordination of the amine to the nickel center. Considering the higher molecular weight of **BPc** (*N,N*-diethyl) relative to **BPb** (*N,N*-dimethyl) it appears that the steric effect must

again be a more critical influence in determining molecular weight than the basicity of aniline.

Examination of Table 3 also shows that the nitro group is tolerated by (η^6 -toluene)Ni(C₆F₅)₂ although once

again the molecular weight of BPe was lower than that prepared in the absence of nitrobenzene, i.e., **HP**. Among these tolerance tests, the successful polymerizations in the presence of nitro, *N,N*-dimethyl, *N,N*-diethyl, and *N,N*-diphenyl units were very encouraging because many NLO chromophores contain these same structure units. On the basis of this preliminary examination, we deduce that the nickel catalyst tolerance order (related to the molecular weight of polymer produced) involving the following nitrogen-containing functional groups is as follows: $-\text{NPh}_2 > \text{NEt}_2 > \text{NMe}_2 > \text{NO}_2 \gg \text{NH}_2 \sim \text{CN}$.

As a next functional group tolerance test for the nickel catalyst blend polymerizations in the presence of 20 mol % of various *N,N*-diethyl-substituted NLO chromophores were carried out. These guest compounds are all diethylanilines that contain additional acceptor functional groups such as nitro, aldehyde, cyano, dicyano, and ketone in the para position (Table 4). Just as in the case of the first blend polymerization study (Table 3), all polymerizations attempted on cyano group containing monomers (**BPj** and **BPk**) failed. On the basis of the results already described (Table 3), we expected that an electron-withdrawing nitro group would decrease the basicity of aniline so that **BPi** might be obtained with a higher M_w than **BPg**. However, the outcome revealed that the *N,N*-diethyl group and nitro group give a still lower M_w than **BPg** and this indicates again that the relative basicity of the aniline does not appear to be a significant influence. Nevertheless, the polymerization **BPi** containing the nitro-substituted aniline gave a poly(norbornene) of M_w 276 000 that certainly is high enough for creation of nonlinear optical thin films and therefore a very promising result. It was also found that the aldehyde functional group lowered the M_w of the polymer much more than a ketone functional group (at least relative to the type of ketone found in indanedi-one). On the basis of this preliminary examination, we deduce that the nickel catalyst tolerance order (related to the molecular weight of polymer produced) for the following functional groups is: $\text{ArC=O} > \text{NO}_2 > \text{CHO} \gg \text{CN} \sim \text{C=C(CN)}_2$. Although the ketone functional group was preferable to the nitro group for obtaining a high M_w of poly(norbornene), the latter group appears more attractive considering it is a better electron acceptor for higher NLO susceptibility. Thus far, the nitro group appears to be the most practical acceptor for NLO chromophores involved in polymerizations using this nickel-initiated process.

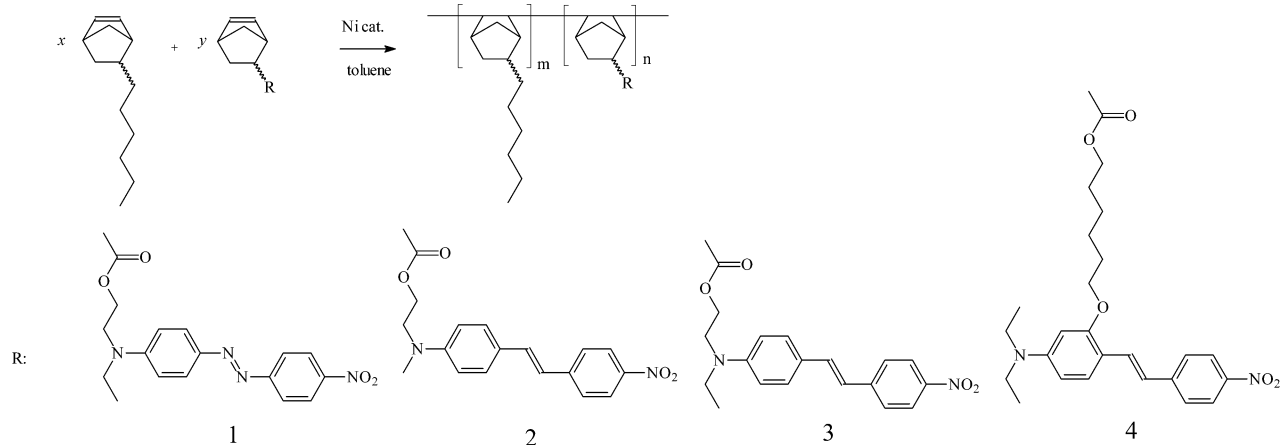
Copolymerization. With the knowledge that the nickel catalyst tolerated both tertiary amine and nitro functional groups, we examined the conditions for copolymerization of hexylnorbornene with the norbornene functionalized DR1-based monomer (**M1**). The feed ratio of two monomers was fixed at 80/20 (mol %/mol %) and the influence of overall monomer concentration on M_w was examined (compare **CP1a–CP1d**, Table 5). The polymerization at 2 mmol monomer in 6 mL of solvent produced the highest M_w of 125 000. More concentrated and more diluted systems produced lower M_w . The optimum catalyst concentration was found to be in the range of 0.5–1.0 mol % (compare **CP1e–CP1h**). When the catalyst concentration was increased above 1 mol % the M_w of copolymer was not increased significantly and so 1 mol % catalyst was sufficient. The standard polymerization conditions for 2 mmol of monomer was found to be 6 mL of toluene, 0.01–0.02 mmol

of Ni catalyst at room temperature for 24 h. In all cases, the gel permeation chromatograms were unimodal consistent with the formation of a copolymer.

With these same reaction conditions kept constant the level of NLO chromophore incorporation into the copolymer (compare **HP–CP11** in Table 5) was examined, i.e., does the composition of the copolymer reflect the original feed ratio of the monomers? It was found that as the chromophore-containing monomer **M1** portion increased both the molecular weights and the yields of the copolymers steeply decreased. At a feed ratio of $x/y = 80/20$ (mol %/mol %) the M_w decreased by an order of magnitude compared to the homopolymer M_w (**HP**). However, a copolymer (**CP1k**) polymerized at a feed ratio as high as 50/50 (mol %/mol %) still had an M_w of 70 000. The DR1 content in copolymers was determined by 500 MHz ^1H NMR spectrometry by normalizing the aromatic resonance at 8.3 ppm (2H) normalized to 1.00 (see Supporting Information). Between a feed ratio of $m/n = 80/20$ –50/50 (mol %/mol %) the n value was in the range of 17–36 mol % and so the actual loading of the NLO chromophore was somewhat lower presumably due to the lower polymerization reactivity of an NLO monomer like **M1** relative to **18**. Considering the higher loading of DR1 chromophore and the film forming capabilities, **CP1i** or **CP1j** may be good candidates for practical production among these copolymers. It is also a promising sign that the two nitrogen atoms in the azo linkage ($-\text{N}=\text{N}-$) did not critically affect the catalyst activity.

Figure 5 shows all the norbornene functionalized monomer structures synthesized in this study and the specific results of copolymerization with hexylnorbornene are summarized in Table 6. All the polymerizations except **CP5–CP9** were carried out on a 2 mmol monomer scale (**13/M1**) of 80/20 (mol %/mol %) and 70/30 (mol %/mol %) feed ratio, respectively. Because of the nickel complex's incompatibility with the cyano group, the feed ratios of polymerization of **CP5–CP9** were decreased to only 95/5 (mol %/mol %). Despite this considerable reduction in concentration of cyano-containing monomers all the polymerization attempts of **CP5–CP9** were unsuccessful indicative of the potent inhibitory effect of the cyano group. The stilbene-based NLO monomers were all successfully copolymerized with **18** to give higher molecular weight NLO polymers (**CP2–CP4**) than the comparable azobenzene-based NLO polymer **CP1** which may be due to a weak inhibitory influence on catalysis by the nitrogen containing π -bridge ($-\text{N}=\text{N}-$) group. The higher M_w of **CP3** compared with **CP2** was due to the steric demands of the *N,N*-diethyl group vs the *N,N*-dimethyl group with smaller alkyl substitution as was demonstrated in the tolerance test. The highest M_w value of **CP4** may be reflected by the bulkier structure of **CP4**, because the molecular weights were measured by size exclusion chromatography.

On the basis of the successful small-scale (2 mmol) polymerization results larger scale polymerizations for the preparation of sufficient material for electrooptical evaluations were run and Table 7 shows the polymerization results (**LCP1–LCP4**). The copolymers were obtained in a 65–75% yield and with M_w 102 000–278 000 as red-orange powders. The molecular weight values reproduced those of the small-scale polymerization quite well. The 500 MHz ^1H NMR spectra of **LCP1–LCP4** are given in the Supporting Information.

Table 7. NLO Copolymerization Scale-up Results^a

no.	R	x/y (mol %/mol %)	yield (%)	m/n (mol %/mol %)	$M_w (\times 10^3)$	$M_n (\times 10^3)$	M_w/M_n
LCP1(8/2)	1	80/20	76	81.2/18.8	123	43	2.90
LCP1(7/3)	1	70/30	65	71.6/28.4	102	38	2.66
LCP2(7/3)	2	70/30	74	69.7/30.3	185	47	3.94
LCP3(7/3)	3	70/30	69	69.1/30.9	191	48	4.01
LCP4(7/3)	4	70/30	73	68.9/31.1	278	75	3.70

^a Polymerization temperature: RT, polymerization time: 24 h. ^b Measured by ¹H NMR spectra.

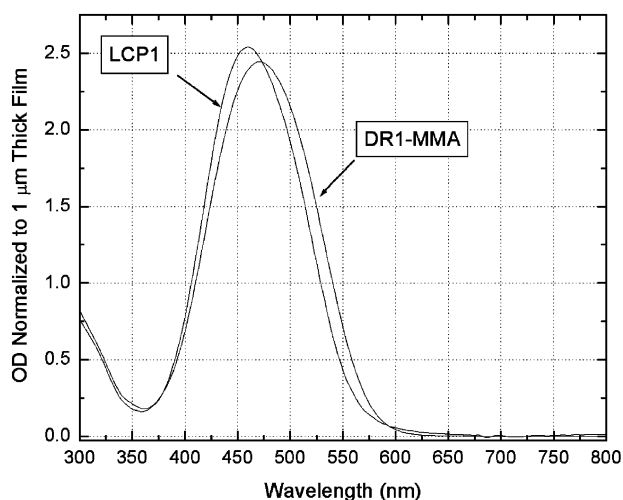


Figure 6. UV-vis spectrum of thin films of DR1-MMA and LCP1.

close to theoretical, by NMR, Table 7) while the DR1-MMA polymer has a 10 mol % monomer feed. Although the mol % of the chromophores differ by a factor of 2 the weight or volume ratio is much closer to one. To make this comparison the **LCP1** polymer was dissected into three parts, the hexylnorbornene comonomer ($C_{13}H_{22}$, MW 137), the norbornene acid part of the ester-containing monomer ($C_8H_9O_2$, MW 137), and, finally, the "active" part 4-diethylamino-4'-nitroazobenzene ($C_{16}H_{18}N_4$, MW 297). The weight or volume percentage of active chromophore in **LCP1** is thus 25.9% given by the ratio $(2 \times 297)/(8 \times 178 + 2 \times 137 + 2 \times 297)$. A comparable analysis for the DR1-MMA polymer was done, and here the polymer containing 10 mol % chromophore monomer was determined to be 23.2% weight or volume active chromophore from the ratio $(1 \times 297)/(9 \times 100 + 1 \times 85 + 1 \times 297)$. So, on volume or weight percentage basis, the two polymers that will be compared here have similar loadings of the same chromophore on a weight or volume basis. The definition of the "active" and "inactive" components of these polymers is somewhat arbitrary, but whatever bias is

involved in the definition applies to both systems. Whenever NLO polymers are compared, especially across different polymer classes, this kind of chromophore loading analysis is required. Different polymer films of equal thickness containing identical chromophores should generate second harmonic signals of equal magnitude if the chromophore loadings are comparable and the extent of chromophore orientation is comparable and the microscopic properties (the $\mu\beta$ products) are comparable. All these contributions have been considered in the following *four sets* of poling experiments that compare DR1-MMA and LCP1.

The *first set* of poling experiments was performed in a poling station without in situ SHG measurements. A total of four films, two DR1-MMA (#1, #2) and two **LCP1** (#3, #4), with thicknesses well below their coherence length were prepared and corona poled. The coherence length is $l_c = (\lambda/2)(1/(n^{2\omega} - n^\omega))$, where λ is the fundamental laser wavelength and n^ω and $n^{2\omega}$ are the refractive indices at the fundamental and second harmonic wavelengths, respectively of DR1-MMA and **LCP1** at 1057 nm are 3.95 and 4.26 μm , respectively. For each film the $P^{2\omega}$ was obtained at two different points during the overall poling process: the first determination of $P^{2\omega}$ is done after cooling to room temperature but prior to removal of surface charge while the second determination of $P^{2\omega}$ is done after elimination of surface charge by immersion of the film in water for 5–10 min. The *first set* of poling experiments was performed in a poling station without in situ SHG measurements. The poling experiments the conditions chosen for **LCP1** were a temperature in the 100–120 °C range, voltage ~ 6 kV and a current in the 3–4 μA range. The ratios of susceptibilities among these four films was calculated from the eq 2 are summarized in Table 8a, while Table 8b shows all the parameters used that are used in the calculation.

In Table 8a the ratio of the effective susceptibilities of the two DR1-MMA films (#1 and #2) before and after removal of surface charge (leading to removal of the field resulting from the surface charge) are both close to 1, indicating that the experimental premise that we can

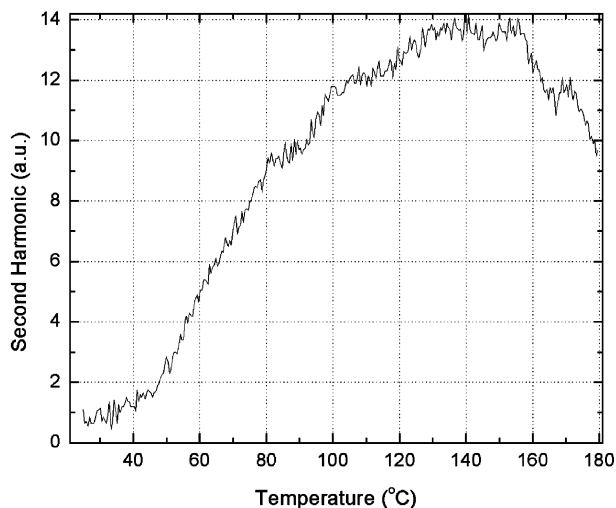
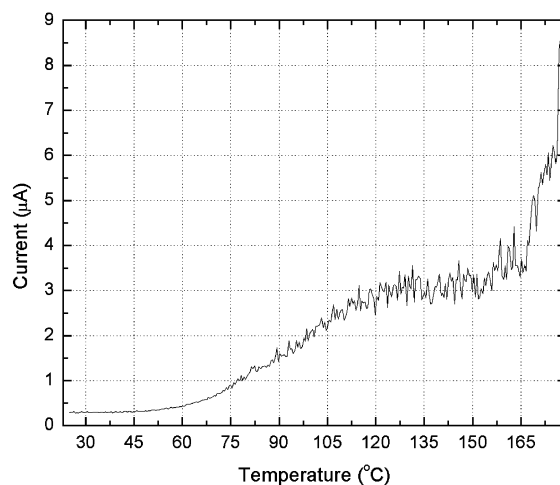
Table 8. Ratio of Susceptibilities and Parameters Used, Where the Subindex Indicates the Film Number

	Ratio of Susceptibilities	
	immediately after poling	after neutralization of surface charge
$\chi_1^{(2)}/\chi_2^{(2)}$	1.06	1.1
$\chi_1^{(2)}/\chi_3^{(2)}$	1.17	2.32
$\chi_1^{(2)}/\chi_4^{(2)}$	1.19	2.01
$\chi_2^{(2)}/\chi_3^{(2)}$	1.12	2.13
$\chi_2^{(2)}/\chi_4^{(2)}$	1.13	1.68

Parameters Used for Calculation of Susceptibility Ratios				
film no.	EOP	L (nm)	P^ω (mW)	$P^{2\omega}$ (au)
1	DR1-MMA	430	590	13.9
2	DR1-MMA	500	610	17
3	LCP1	455	590	2.9
4	LCP1	415	590	3.2

pole DR1-MMA in a repeatable manner is correct. However, and in contrast, the effective second-order nonlinear optical susceptibility ratios between the DR1-MMA films (#1 and #2) and LCP1 films (#3 and #4) are all around 1 before water treatment but closer to 2 after water treatment. In DR1-MMA only a small reduction in the effective second-order susceptibility occurs upon removal of surface charge (on the order of 10%) while in the LCP1 films this reduction in the effective second order susceptibility is much larger (on the order of 50%) upon removal of the surface charge. A change (reduction) in the effective susceptibility can occur upon removal of surface charge due to (at least) two contributions: first, when the surface charge is removed then the EFISH contribution is eliminated and, second, if the nonlinear molecular dipoles are not firmly held by the polymer matrix then dipoles may relax to a less ordered orientation. Ideally, when the surface charges are removed the polymer matrix should hold the dipole orientation and only the EFISH contribution would be eliminated. The results of this experiment indicates that in comparison with DR1-MMA, in LCP1 this "chromophore trapping in the polymer matrix" is not nearly as effective as it should be, resulting in additional dipolar relaxation.

Because of these very unusual chromophore relaxation results with LCP1 a *second set* of poling experiments were repeated using an in situ device so that the optimum poling temperature could be better observed by direct determination of the SHG signal. These in situ experiments are intended only to identify the most advantageous conditions to obtain maximum $P^{2\omega}$ but not to determine absolute or even relative $\chi^{(2)}$ values. The suspicion here was that in the first set of measurements that the poling for LCP1 was not performed in the appropriate glass transition region so this second in situ SHG experiment as a function of temperature was performed. For the in situ poling studies a 2.4 μm thick film of LCP1 polymer was spin-coated onto the backside of 0.8 mm thick ITO-coated substrates. After spinning, the film was baked for > 12 h in a vacuum oven at 100 $^\circ\text{C}$, and after cooling, the film was mounted in the in situ device. The corona discharge was performed with a fixed voltage of 5 kV. The film was gradually heated while the SHG and poling current were measured. As can be seen in Figure 7 for a fixed poling voltage the SH signal grows steadily as temperature increases from ambient to about 140 $^\circ\text{C}$, then a broad maximum of about 14 au is obtained around 140–160 $^\circ\text{C}$ and then finally the SH signal diminishes above 160 $^\circ\text{C}$. Likewise,

**Figure 7.** SHG as a function of temperature for the LCP1 nonlinear optical polymer.**Figure 8.** Poling current as a function of temperature for the LCP1 nonlinear optical polymer.

in Figure 8 it can be seen that the current through this same film gradually increases as the temperature is raised between ambient and 160 $^\circ\text{C}$ and then rises abruptly above 160 $^\circ\text{C}$. In other polymers studied previously this simultaneous drop in SHG and rise in poling current at a common temperature is the signature of a glass transition. As the glass transition is approached the chromophore mobility and the ability to align in response to the field both increase. However, the ionic mobility rises simultaneously and the increased current ultimately compromises the magnitude of the electric field across the film. For this reason, and because the poling efficiency always contains a component that is inversely proportional to kT , there is no advantage in raising the poling temperature still further.

From this *second set* of in situ experiments on LCP1 just described it appears that the glass transition of this poly(norbornene) might be higher than the poling temperature used in the *first set* of experiments. So, after the in situ poling studies we hoped to verify that at a 160 $^\circ\text{C}$ poling temperature we might now be able to better pole LCP1 and on cooling to more effectively "lock" the oriented chromophore in the matrix. For the follow up *third set* of experiments an approximately 1:1 solution (0.2 μm filtered) of LCP1 in 1,1,1,2-tetrachloroethane was spin-coated on a 1 mm thick sodalime

glass substrate at 4000 rpm. After baking in a vacuum for approximately 12 h this new film 5 had a thickness of 455 nm that is well below its coherence length (4.26 μm). This film was poled for 30 min in the poling station at the "optimal" temperature of 160 °C using 5.9 kV poling voltage and $2.6 \pm 0.2 \mu\text{A}$ poling current. The poling voltage was determined using the in situ cell by observing the growth of second harmonic signal as the poling voltage is raised to a point where the growth stops. Just as in the case of films 1–4 after the optimum poling parameters have been determined in the in situ cell the poling station is used because it can provide poling parameters that can be controlled more accurately. After exposure to elevated temperature and high voltage this film was allowed to gradually cool over approximately 2 h while the high voltage was sustained. Immediately after poling (and prior to immersion of the film in water) a second harmonic signal of 11.8 au was measured. However, after 5 min of immersion in DI water, a second harmonic signal of 3.2 au was measured for the same film at the same fundamental laser power and PMT voltage. The ratio of effective second-order nonlinear optical susceptibility is therefore 0.51, which is consistent with the *first set* of poling experiments where this ratio, calculated from Table 8a, is 0.57 ± 0.08 . These results indicate that "locking" of the chromophore in the **LCP1** polymer backbone matrix was not achieved even after poling at the higher poling temperatures of 160 °C.

Finally, an additional *fourth set* of experiments were devised, in this case to evaluate the relative room temperature mobility of the DR1 chromophore when it is incorporated in the PMMA and poly(norbornene) systems. In this fourth experiment, previously unpoled (isotropic) films of both DR1-MMA and LCP1 are maintained at room temperature under the influence of a corona discharge electric field. Any SH signal that results will be due only to EFISH if the molecules cannot reorient, but if there is some freedom for molecular rotation at room temperature (and well below T_g of either polymer), then an electrooptic component will also contribute to SHG. Here, a 3.9 μm film of LCP-1 and a 4.0 μm film of DR1-MMA were spin-coated on the uncoated surface of a ITO-coated glass substrates. The film thickness for the films is almost identical. Both films were baked under vacuum at 100 °C for a period of at least 24 h. The films were mounted in the in situ poling cell, and at room temperature a 5 kV voltage was applied producing a current of less than 0.2 μA . Prior to the conduction of an experimental run it was verified that the electrical poling conditions were identical for both films. The SH signal was sampled every 15 s for a period of 3600 s. To avoid any possible photodegradation damage to the chromophore (this is only a precautionary measure as we do not have any evidence of degradation) due to the long duration of the experiment, a laser power lower than the first three sets of experiments was used and the laser was blocked by a shutter that periodically opened only for 2 s (enough time for the lock-in to settle).

The results of this *fourth* experiment are very clear from examination of Figure 9. During the first 500 s of poling the signals from DR1-MMA and LCP1 are comparable. The second harmonic signal does not increase instantaneously because the corona-discharge poling configuration has a large time constant due to large product of the effective resistance and effective capacitance. While the mobility of the chromophore in

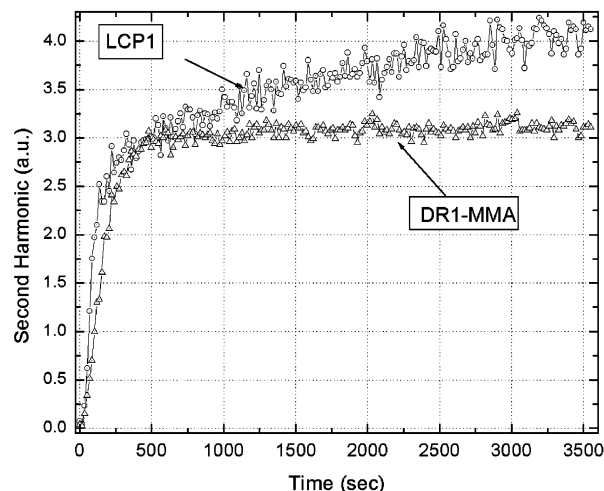


Figure 9. SHG obtained from previously unpoled DR1-MMA and **LCP1** films under the influence of a 5 kV corona-poling field at room temperature.

the host does play a role in this regime, its signal strength is dominated by the charge build-up on the film. However, after the initial large growth of second harmonic signal the LCP1 film the signal continues to increase and during the 3500 s duration of the experiment it never reaches a stable level, while the DR1-MMA signal plateaus after the initial large growth. This implies that in the case of **LCP1** that either the electric field continues to increase and/or the chromophore reorientation is taking place in **LCP1** at room temperature (and indicative of chromophore mobility even well below the apparent T_g). While there certainly are differences in the dielectric properties of DR1-MMA and **LCP1**, one does not expect them to be so different as to explain the difference in the electric field build-up. While it is known that a chromophore can be mobile well below the glass-transition temperature,²⁷ it is of interest here that the same chromophore is much more mobile in the poly(norbornene) host than in the methacrylate host, indicative of the existence of more free-volume in the poly(norbornene). This experiment corroborates the idea that chromophore polar order relaxation is the source of the large orientation decay seen in freshly poled DR1-norbornene samples after immersing them in DI water. The greater chromophore mobility in the norbornene system leads to loss of chromophore orientation after the residual charges introduced by the poling procedure are removed.

From these experiments, we observed that the poly(norbornene) matrix in **LCP1** behaves quite differently than the methacrylate matrix in DR1-PMMA and, in fact, quite differently from any other polymers in our experience. The reasons for this behavior is not yet fully understood; however, we conjecture that at the higher temperature that the void space is not filled in the **LCP1** polymer, and this makes it easier for the reorientation of the nonlinear chromophore in the absence of an electric field upon cooling and removal of surface charges.

Conclusions

In this study, we have adopted the addition polymerization of norbornenes as a method for the preparation of electroactive polymers, in particular polymers designed as electrooptical materials. Synthetic pathways have been developed that permit the introduction of the

reactive functionality, a norbornene ring, into a wide range of second-order nonlinear optical chromophores. The polymerization of these norbornene-functionalized monomers with a nickel catalyst has been examined and with the help of guest–host model systems the tolerance of the nickel catalyst to typical chromophore acceptor and donor functional groups has been determined. In the case of a hexylnorbornene and DR1 containing material, the synthesis was successfully scaled up to the multigram level to give an amino–nitro-substituted azobenzene material **LCP1** with good film forming and other good ancillary properties for NLO application. Preliminary measurements of SHG in this poly(norbornene) material indicate that it can be poled just like a conventional system such as DR1-MMA but that the poled order stability appears to suffer from enhanced relaxation. The polar order relaxation in **LCP1** was studied in some detail including a room-temperature poling experiment which may be of general utility for evaluation of poled order stability in polymers. The relaxation phenomena found in **LCP1** needs to be examined in other related norbornene systems to see if it is very general. If so, subsequent studies to mitigate (or possibly exploit) this relaxation may be required.

Acknowledgment. The investigations at Promerus LLC (formerly BFGoodrich Electronic Materials) and Kent State University were supported by an Advanced Technology Program grant from the National Institute of Standards and Technology (ATP Project 98-02-0023). This work at UC Davis was supported in part by the MRSEC Program of the National Science Foundation under Award DMR-9808677 for CPIMA II.

Supporting Information Available: Text giving the synthesis of norbornene monomers M1–M9 and figures showing NMR spectra of norbornene copolymers. This material is available free of charge via the Internet at <http://pubs.acs.org>.

References and Notes

- (1) (a) Dalton, L. *Polym. Photonics Appl.* **2002**, *158*, 1–86. (b) Eldada, L. *Opt. Eng.* **2001**, *40*, 1165–1178.
- (2) (a) Hubbard, M. A.; Marks, T. J. *Chem. Mater.* **1992**, *4*, 965. (b) Shi, Y.; Steier, W. H.; Chen, M.; Yu, L. P.; Dalton, L. R. *Appl. Phys. Lett.* **1992**, *60*, 2577. (c) Wu, J. W.; Valley, J. F.; Ermer, S.; Binkley, E. S.; Kenney, J. T.; Lipscomb, G. F.; Lytel, R. *Appl. Phys. Lett.* **1991**, *58*, 225. (d) Mandal, B. K.; Chen, Y. M.; Lee, J. Y.; Kumar, J.; Tripathy, S. *Appl. Phys. Lett.* **1991**, *58*, 2549.
- (3) Laschewsky, A.; Schulzhanke, W.; *Makromol. Chem. Rapid Commun.* **1993**, *14*, 683–691.
- (4) Grubbs, R. H.; Gorman, C. B.; Ginsburg, E. J.; Marder, S. R.; Perry, J. W. *Abstr. Pap. Am. Chem. Soc.* **1990**, *199*, 345-INOR, Part 1.
- (5) (a) Maughon, B. R.; Weck, M.; Mohr, B.; Grubbs, R. H. *Macromolecules* **1997**, *30*, 257. (b) Weck, M.; Mohr, B.; Maughon, B. R.; Grubbs, R. H. *Macromolecules* **1997**, *30*, 6430.
- (6) (a) Lee, J.-K.; Schrock, R. R.; Baigent, D. R.; Friend, R. H. *Macromolecules* **1995**, *28*, 1966. (b) Boyd, T. J.; Geerts, Y.; Lee, J.-K.; Fogg, D. E.; Lovoie, G. G.; Schrock, R. R. *Macromolecules* **1997**, *30*, 3553. (c) Bellmann, E.; Shaheen, S. E.; Thayumanavan, S.; Barlow, S.; Grubbs, R. H.; Marder, S.; Kippelen, B.; Peyghambarian, N. *Chem. Mater.* **1998**, *10*, 1668.
- (7) Thorn-Csanyi, E.; Kraxner, P.; Strachota, A. *Macromol. Rapid Commun.* **1998**, *19*, 223–228.
- (8) (a) Sartori, G.; Ciampelli, F.; Cameli, N. *Chim. Ind. (Ital.)* **1963**, *45*, 1479. (b) McKeon, J. E.; Starcher, P. S. US Patent 3,330,815, 1967.
- (9) Much of the work of Kaminsky, Sen, Risse, Heitz, Novak, Arndt, and Goodall has been reviewed recently. (a) Janiak, C.; Lassahn, P. G. *J. Mol. Catal. A: Chem.* **2001**, *166*, 193. (b) Janiak, C.; Lassahn, P. G. *Macromol. Rapid Commun.* **2001**, *22*, 479–492. (c) Goodall, B. L. In *Late Transition Metal Polymerization Catalysis*; Rieger, B., Saunders Baugh, L., Kacker, S., Striegler, S., Eds.; Wiley-VCH: Weinheim, Germany, 2003.
- (10) (a) Arndt, M.; Gosmann, M. *Polym. Bull. (Berlin)* **1998**, *41*, 433. (b) Arndt, M.; Kaminsky, W. *Macromol. Symp.* **1995**, *97*, 225.
- (11) (a) Goodall, B. L.; Benedikt, G. M.; McIntosh, L. H., III; Barnes, D. A. US Patent 5,468,819, 1995. (b) Goodall, B. L.; Benedikt, G. M.; McIntosh, L. H., III; Barnes, D. A.; Rhodes, L. F. US Patent 5,569,730, 1996. (c) Goodall, B. L.; Risse, W.; Mathew, J. P. US Patent 5,705,503, 1996. (d) Goodall, B. L.; Benedikt, G. M.; McIntosh, L. H., III; Barnes, D. A.; Rhodes, L. F. *Proc. Am. Chem. Soc. Div. Polym. Mater.: Sci. Eng.* **1997**, *76*, 56. (e) Goodall, B. L.; Benedikt, G. M.; McIntosh, L. H., III; Barnes, D. A.; Rhodes, L. F. *Polym. Prepr. (Am. Chem. Soc., Div. Polym. Chem.)* **1998**, *39*(1), 216.
- (12) Ivin, K. J.; Mol, J. C. *Olefin Metathesis and Metathesis Polymerization*; Academic Press: San Diego, CA, 1997; p 407.
- (13) Barnes, D. A.; Benedikt, G. M.; Goodall, B. L.; Hullihen, K.; Jayaraman, S.; McDougall, W. C.; McIntosh, L. H., III; Rhodes, L. F.; Shick, R. A. *Proceedings of MetCon 98 (Worldwide Metallocene Conference)*; Catalyst Consultants Inc.: Houston, TX, 1998.
- (14) (a) Kim, J. M.; Shin, H. Y.; Park, K. H.; Kim, T. H.; Ju, S. Y.; Han, D. K.; Ahn, K. D. *Macromolecules* **2001**, *34*, 4291. (b) Kang, S. H.; Shin, H.-D.; Oh, C.-H.; Choi, D. H.; Park, K. H. *Bull. Korean Chem. Soc.* **2002**, *23*, 957.
- (15) Rhodes, L. F.; Bell, A.; Jayaraman, S.; Lipian, J.-H.; Goodall, B. L.; Shick, R. A. US Patent 6,232,417, 2001.
- (16) Pretre, Ph.; Wu, L. M.; Hill, R. A.; Knoesen, A. *Opt. Soc. Am. B* **1998**, *15*, 379.
- (17) Singer, K. D.; Lalama, S. L.; Sohn, J. E.; Small, R. D. *Electrooptic Organic Materials*, Chapter II-8. In *Nonlinear Optical Properties of Organic Molecules and Crystals*; Chems, D. S., Zyss, J., Eds.; Academic Press: 1987; Volume 1.
- (18) Knoesen, A. Chapter 9: Photoisomerization in Polymer Films in the Presence of Electrostatic and Optical Fields. In *Photoreactive Organic Thin Films*; Sekkat, Z., Knoll, W., Eds.; Academic Press: Amsterdam, 2002.
- (19) Lupu, D.; Ringsdorf, H.; Schuster, A.; Seitz, M. *J. Am. Chem. Soc.* **1994**, *116*, 10498.
- (20) *Characterization Techniques and Tabulations for Organic Nonlinear Optical Materials*; Kuzyk, M. G., Dirk, C. W., Eds.; Marcel-Dekker: New York, 1998.
- (21) *Polymers for Photonics Applications I: Nonlinear Optical and Electro Luminescence Polymers*; Advances in Polymer Science 158; Lee, K.-S., Ed.; Springer-Verlag: 2002.
- (22) Robello, D. R.; Dao, P. T.; Schildkraut, J. S.; Scozzafava, M.; Urankar, E. J.; Wiland, C. S. *Chem. Mater.* **1995**, *7*, 284–291.
- (23) Prime, R. B.; Chiou, G. Y.; Twieg, R. J. *J. Therm. Anal.* **1996**, *46*, 1133–1150.
- (24) Slessor, K. N. *Can. J. Chem.* **1971**, *49*, 2874.
- (25) Robinson, B. H.; Dalton, L. R.; Harpe, A. W.; Ren, A.; Wang, F.; Zhang, C.; Todorova, G.; Lee, M.; Aniszfeld, R.; Garner, S.; Chen, A.; Steier, W. H.; Houbrecht, S.; Persoons, A.; Ledoux, I.; Zyss, J.; Jen, A. K. Y. *Chem. Phys.* **1999**, *245*, 35–50.
- (26) (a) Lopez, G.; Garcia, G.; Sanchez, G.; Garcia, J.; Ruiz, J.; Hermoso, J. A.; Vegas, A.; Martinez-Ripoll, M. *Inorg. Chem.* **1992**, *1*, 1518. (b) De Haro, C.; Garcia, G.; Sanchez, G.; Lopez, G. *J. Chem. Res., Synop.* **1986**, *4*, 119. (c) Falvello, L. R.; Fornies, J.; Navarro, R.; Sicilia, V.; Tomas, M. *J. Chem. Soc.; Dalton Trans.* **1994**, *12*, 3143. (d) Falvello, L. R.; Fornies, J.; Navarro, R.; Sicilia, V.; Tomas, M. *Angew. Chem.* **1990**, *102*, 952.
- (27) Sekkat, Z.; Pretre, P.; Knoesen, A.; Volksen, W.; Lee, V. Y.; Miller, R. D.; Wood, J.; Knoll, W. *J. Opt. Soc. Am. B* **1998**, *15*, 401–413.

MA040044I